

# Weak interference between the $1^-$ states in the vicinity of $\alpha$ -particle threshold of $^{16}\text{O}$

M. Katsuma<sup>1,2</sup>

<sup>1</sup> Advanced Mathematical Institute, Osaka City University, Japan,

<sup>2</sup> Institut d'Astronomie et d'Astrophysique, Université Libre de Bruxelles, Belgium

**Abstract.** The subthreshold  $1_1^-$  state at an excitation energy  $E_x = 7.12$  MeV in  $^{16}\text{O}$  has been believed to enhance the  $S$ -factor of  $^{12}\text{C}(\alpha,\gamma)^{16}\text{O}$ . The enhancement seems to originate from strong interference between  $1_1^-$  and  $1_2^-$  ( $E_x \approx 9.6$  MeV) in the vicinity of the  $\alpha$ -particle threshold. However, weak interference between them and a resulting small  $E1$   $S$ -factor are exemplified with  $R$ -matrix theory. Including a higher-order correction of the resonance parameters, the present example appears to reproduce the experimental data consistently. It would therefore be possible that the  $E1$   $S$ -factor is reduced at low energies.

**Keywords:**  $^{12}\text{C}(\alpha,\gamma)^{16}\text{O}$ ,  $R$ -matrix method, Stellar nucleosynthesis

The  $1_1^-$  ( $E_x = 7.12$  MeV) and  $1_2^-$  ( $E_x \approx 9.6$  MeV) states in  $^{16}\text{O}$  play an important role in the low-energy extrapolation of  $^{12}\text{C}(\alpha,\gamma)^{16}\text{O}$  cross sections. If complicated process of compound nuclei is assumed, strong interference between them is expected, and  $E1$  transition becomes predominant. At present, this interference has been believed to describe the cross section at  $E_{c.m.} = 300$  keV. However, I have predicted a small  $E1$   $S$ -factor at this energy from the potential model (PM) [1], because non-absorptive scattering results in weak coupling between shell and cluster structure in  $^{16}\text{O}$ . Besides, I have shown that  $E2$  transition is dominant because  $2_1^+$  ( $E_x = 6.92$  MeV) has  $\alpha+^{12}\text{C}$  structure [2,3].

In this paper, weak interference between  $1_1^-$  and  $1_2^-$ , and the resulting small  $E1$   $S$ -factor are exemplified with  $R$ -matrix theory [4]. I estimate their reduced  $\alpha$ -particle widths from [1,2], and use the conventional  $R$ -matrix method [5,6]. In addition, the formal parameters are obtained from an exact expression, including a higher-order correction, because it has been reported that the parameters for  $1_2^-$  are not appropriately treated in the linear approximation [5]. This correction ensures that  $R$ -matrix calculations correspond to the experimental data.

Before showing an example of calculations, let me describe the  $R$ -matrix parameters. The Schrödinger equation is solved with the  $R$ -matrix,

$$R_L(E_{c.m.}) = \sum_n \frac{\tilde{\gamma}_{nL}^2}{\tilde{E}_{nL} - E_{c.m.}} + \mathcal{R}_{\alpha L}, \quad (1)$$

where  $\mathcal{R}_{\alpha L}$  is the non-resonant component.  $\tilde{E}_{nL}$  and  $\tilde{\gamma}_{nL}$  are the *formal* resonance energy and *formal* reduced width, respectively. These are different from the Breit-Wigner (observed) parameters,  $E_{nL}$ ,  $\gamma_{nL}$ . The conversion is given as

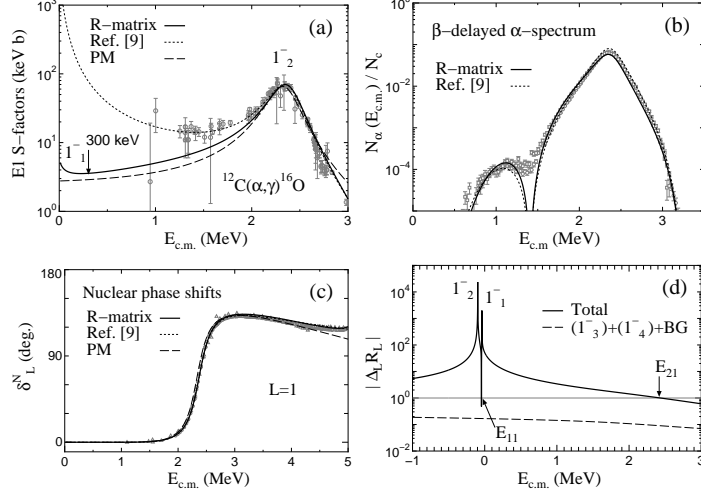


**Fig. 1.** An example of  $R$ -matrix calculations of (a)  $E1$   $S$ -factor of  $^{12}\text{C}(\alpha,\gamma)^{16}\text{O}$ , (b)  $\beta$ -delayed  $\alpha$ -particle spectrum of  $^{16}\text{N}$ , (c)  $p$ -wave phase shift of  $\alpha+^{12}\text{C}$  elastic scattering. The solid, dotted, and dashed curves are the results of the present work,  $R$ -matrix method [9], and PM [1], respectively. The experimental data are taken from [9,10,11]. (d) The resultant  $R$ -matrix is illustrated with the solid curve. The dashed curve is the sum of  $1_3^-$ ,  $1_4^-$ , and non-resonant components.

$$\tilde{E}_{nL}(E_{c.m.}) = E_{nL} + \tilde{\gamma}_{nL}^2(E_{c.m.})\Delta_L(E_{nL}, a_c) [1 + d_{nL}] \quad (2)$$

$$\tilde{\gamma}_{nL}^2(E_{c.m.}) = \frac{\gamma_{nL}^2}{1 - \gamma_{nL}^2 \Delta'_L(E_{nL}, a_c) [1 + Q_{nL}(E_{c.m.}, a_c)]}, \quad (3)$$

where  $Q_{nL}$  is the higher-order correction of the resonance parameters, depending on energies. Note that  $Q_{nL} = 0$  was used in most of reactions [5,6].  $\Delta_L$  is the shift function,  $\Delta'_L = d\Delta_L/dE$ .  $d_{nL}$  is a parameter for multi-levels, and it is adjusted self-consistently so as to satisfy  $\Delta_L(E_{nL}, a_c)R_L(E_{nL}) = 1$ ;  $d_{11} = -1.0133$ ,  $d_{21} = 0$ . The observed parameters are  $1_1^-$ :  $E_{11} = -0.0451$  MeV,  $\gamma_{11} = 0.345$  MeV $^{1/2}$ ;  $1_2^-$ :  $E_{21} = 2.434$  MeV,  $\gamma_{21} = 0.850$  MeV $^{1/2}$ .  $a_c$  is the channel radius,  $a_c = 4.75$  fm. All nucleons are interacting close together in the internal region, whereas nucleons are well-separated into  $\alpha$  and  $^{12}\text{C}$  outside the region. Other observed parameters are taken from [7]. ANC of  $1_1^-$  is  $5.0 \times 10^{28}$  fm $^{-1}$  [1,8].

The example of the small  $E1$   $S$ -factor is shown by the solid curve in Fig. 1(a). The present example includes the component of the subthreshold state, and it resembles PM [1] (dashed curve). The interference between  $1_1^-$  and  $1_2^-$  appears to be weak. The corresponding calculations of the  $\beta$ -delayed  $\alpha$ -particle spectrum of  $^{16}\text{N}$  and the  $p$ -wave phase shift of  $\alpha+^{12}\text{C}$  elastic scattering are consistent with the experimental results [9,10]. (Fig. 1(b) and 1(c)) So, the small  $E1$   $S$ -factor in Fig. 1(a) is in agreement with these experimental data. The experimental  $\alpha$ -particle width of  $1_2^-$  ( $\Gamma_\alpha^{\text{exp}} = 420 \pm 20$  keV [7]) is also reproduced by the present

example,  $\Gamma_\alpha^{\text{th}} = 432$  keV. The dotted curves are the  $R$ -matrix calculations [9] with  $Q_{nL} = 0$ , in which the narrow reduced widths are assumed. The derived  $1_2^-$  width [9] does not reproduce the experimental one. Compared with the solid curves,  $Q_{nL}$  is found to reduce the  $E1$   $S$ -factor at low energies. In fact, a large energy shift for  $1_2^-$  is expected from the large reduced width of  $\alpha+^{12}\text{C}$  cluster structure. (Eq. (2)) So, the resultant energy of the  $1_2^-$  pole is found to be located in the vicinity of  $1_1^-$ . (Fig. 1(d)) This proximity of the poles suppresses their interference, and it consequently makes the small  $E1$   $S$ -factor below the barrier.

The present example can be replaced with my previous result from PM, so I could use a hybrid model [12],  $E1(R\text{-matrix})+E2(\text{PM})$ . The resulting total  $S$ -factor and reaction rates are confirmed to be concordant with [1,13].

In summary, the weak interference between  $1_1^-$  and  $1_2^-$ , and the small  $E1$   $S$ -factor have been exemplified with  $R$ -matrix theory. The formal parameters are obtained from the exact expression, including the higher-order correction. The reduced  $\alpha$ -particle widths of  $1_1^-$  and  $1_2^-$  are estimated from PM. The present example is consistent with the experimental results of the  $\beta$ -delayed  $\alpha$ -spectrum of  $^{16}\text{N}$ , the  $p$ -wave phase shift, and the  $\alpha$ -decay width of  $1_2^-$ . In the example, the pole energy of  $1_2^-$  is located in the vicinity of  $1_1^-$ . This proximity suppresses their interference, and it makes the small  $E1$   $S$ -factor below the barrier. It would therefore be possible in the  $R$ -matrix method that the  $E1$   $S$ -factor is reduced from the enhanced value currently expected. At the same time, the reaction rates are confirmed to be obtained from the direct-capture mechanism [1,13].

I am grateful to Prof. S. Kubono for his comments. I also thank M. Arnould, A. Jorissen, K. Takahashi, H. Utsunomiya, Y. Ohnita, and Y. Sakuragi for their hospitality at Université Libre de Bruxelles and Osaka City University.

## References

1. Katsuma, M.: Phys. Rev. C **78**, 034606 (2008); *ibid.* **81**, 029804 (2010); *ibid.* **90**, 068801 (2014); Proc. of NIC XIV, JPS Conf. Proc. **14**, 021009 (2017).
2. Katsuma, M.: Phys. Rev. C **81**, 067603 (2010); J. Phys. G **40**, 025107 (2013); EPJ Web of Conferences **66**, 03041 (2014).
3. Fujiwara, Y., *et al.*: Prog. Theor. Phys. Suppl. **68**, 29 (1980) and references therein.
4. Katsuma, M.: arXiv:1701.02848 [nucl-th].
5. Descouvemont, P.: Theoretical Models for Nucl. Astrophysics. Nova Science (2003).
6. Thompson, I.J., Nunes, F.: Nuclear Reactions for Astrophysics. Cambridge Univ. Press (2009); Lane, A.M., Thomas, R.G.: Rev. Mod. Phys. **30**, 257 (1958).
7. Tilley, D.R., Weller, H.R., Cheves, C.M.: Nucl. Phys. A **564**, 1 (1993).
8. Oulebsir, N., *et al.*: Phys. Rev. C **85**, 035804 (2012); Brune, C.R., *et al.*: Phys. Rev. Lett. **83**, 4025 (1999); Belhout, A., *et al.*: Nucl. Phys. A **793**, 178 (2007).
9. Azuma, R.E., *et al.*: Phys. Rev. C **50**, 1194 (1994).
10. Tang, X.D., *et al.*: Phys. Rev. C **81**, 045809 (2010); Plaga, R., *et al.*: Nucl. Phys. A **465**, 291 (1987); Tischhauser, P., *et al.*: Phys. Rev. C **79**, 055803 (2009).
11. Kunz, R., *et al.*: Phys. Rev. Lett. **86**, 3244 (2001); Assunção, M., *et al.*: Phys. Rev. C **73**, 055801 (2006); Plag, R., *et al.*: *ibid.* **86**, 015805 (2012); Ouellet, J.M.L., *et al.*: *ibid.* **54**, 1982 (1996); Makii, H., *et al.*: *ibid.* **80**, 065802 (2009).
12. Langanke, K., Koonin, S.E.: Nucl. Phys. A **439**, 384 (1985); *ibid.* **410**, 334 (1983).
13. Katsuma, M.: Astrophys. J. **745**, 192 (2012); PoS (NIC XIII) 106 (2015).